Published in final edited form as:
Dev Cell. 2014 October 13; 31(1): 100–113. doi:10.1016/j.devcel.2014.08.005.

Su(H)-Mediated Repression Positions Gene Boundaries along the Dorsal-Ventral Axis of *Drosophila* Embryos

Anil Ozdemir[1], **Lijia Ma**[2], **Kevin P. White**[2], and **Angelike Stathopoulos**[1,*]

[1]Division of Biology and Biological Engineering, California Institute of Technology, Pasadena, CA 91125 USA

[2]Institute for Genomics and Systems Biology and Department of Human Genetics, University of Chicago, Chicago, IL 60637 USA

SUMMARY

In *Drosophila* embryos, a nuclear gradient of the Dorsal transcription factor directs differential gene expression along the dorsoventral (DV) axis, translating it into distinct domains that specify future mesodermal, neural, and ectodermal territories. However, the mechanisms used to differentially-position gene expression boundaries along this axis are not fully understood. Here using a combination of approaches including mutant phenotype analyses and chromatin-immunoprecipitation, we show that the transcription factor Suppressor of Hairless [Su(H)] helps define dorsal boundaries for many genes expressed along the DV axis. Synthetic reporter constructs also provide molecular evidence that Su(H) binding sites support repression and act to counterbalance activation through Dl and the ubiquitous activator Zelda. Our study highlights a role for broadly-expressed repressors, like Su(H), and organization of transcription factor binding sites within *cis*-regulatory modules as important elements controlling spatial domains of gene expression, to facilitate flexible positioning of boundaries across the entire DV axis.

Keywords

Suppressor of Hairless; Dorsal; Zelda; Snail; gene expression; synthetic reporter; chromatin immunoprecipitation; developmental patterning; *Drosophila melanogaster*; repression; boundary formation; *cis*-regulatory modules

INTRODUCTION

During early embryogenesis, proper positioning of gene expression boundaries is essential as these domains support the progression of gastrulation and the differentiation of distinct

*Corresponding author: angelike@caltech.edu; phone: 626-395-5855.

Accession Numbers

The Su(H) ChIP-seq data have been deposited to the NCBI's GEO database and are available through accession number GSE59726.

tissue types (rev. in Rogers and Schier, 2011; Stathopoulos and Levine, 2004). In the early *Drosophila* embryo, genes are differentially expressed along the dorsoventral (DV) axis and subsequently specify whether a domain becomes mesodermal, neural, or ectodermal. Despite the fact that in most cases sharp borders separate these domains, it remains unclear how the distinct boundaries are positioned (rev. in Reeves and Stathopoulos, 2009; Stathopoulos and Levine, 2005a). Combined input from transcriptional activators and repressors is thought to be important in specifying different domains of expression. For example, the role of repressors in specifying the ventral gene expression boundaries is well established (e.g. Cowden and Levine, 2003; Ip et al., 1992a). However, only limited evidence exists to support a role for repressors in defining dorsal boundaries. As a result, most models that explain DV patterning have assumed that these boundaries are concentration-dependent threshold responses to transcriptional activators (Jiang and Levine, 1993; Rushlow and Shvartsman, 2012; Stathopoulos and Levine, 2005a).

A pivotal player in patterning of the DV axis of *Drosophila* embryos is the NF-κB related, Rel-domain transcription factor Dorsal (Dl) (rev. in Hong et al., 2008; Reeves and Stathopoulos, 2009). Dl is present in a nuclear-cytoplasmic gradient along the DV axis with higher levels of the protein present in ventral regions, and lower levels present progressing more dorsally (rev. in Moussian and Roth, 2005; Rushlow and Shvartsman, 2012). The amount of Dl present within nuclei influences levels of gene expression, as does affinity/number of binding sites within target *cis*-regulatory modules (CRMs) and cooperative interactions with other transcription factors. The transcription factors Daughterless (Da), Grainyhead, STAT92E, Suppressor of Hairless [Su(H)], Twist (Twi), and Zelda (Zld) (also known as Viefaltig) have all been shown to play accessory roles in activation of gene expression along the DV axis (Garcia and Stathopoulos, 2011; Jiang and Levine, 1993; Liang et al., 2008; Liberman and Stathopoulos, 2009; Morel and Schweisguth, 2000). Cooperative interactions between these (and possibly other) factors influence expression along the DV axis (rev. in Reeves et al., 2009). For example, Twi is also present in a nuclear gradient, but compared to the Dl gradient it exhibits a steeper decrease in ventrolateral domains of the embryo. Together these factors are thought to regulate expression of target genes in ventral and ventrolateral regions of the embryo (Jiang and Levine, 1993; Markstein et al., 2004; Zinzen et al., 2009). Whereas in dorsolateral regions of the embryo, cooperative interactions between Dl and Zld help to extend gene expression boundaries further dorsally (Liberman and Stathopoulos, 2009; rev. in Rushlow and Shvartsman, 2012).

According to the threshold-response model, dorsal gene boundaries are established by decreasing levels of one or more factors below the required level to support activation (e.g. Jiang and Levine, 1993; Liberman and Stathopoulos, 2009; Rushlow and Shvartsman, 2012). This model does not require input from dorsally acting repressors, and indeed few have been identified. Exceptions include the regulation of the genes *single-minded* (*sim*) and *intermediate neuroblasts defective* (*ind*), which are considered specialized-cases (Morel and Schweisguth, 2000; Stathopoulos and Levine, 2005c). The activity of repressors is challenging to track, because the expansion that occurs in the absence of repressor activity can be subtle.

The *snail* (*sna*) gene encodes a zinc-finger transcriptional repressor that acts to restrict neuroectoderm and neural fate from the invaginating mesoderm (Ip et al., 1992c; Kasai et al., 1992). Several studies have invoked repressive-activity in specification of the sharp expression boundary associated with *sna* (Dunipace et al., 2011; Huang et al., 1997). Early studies focusing on a promoter-proximal *sna* CRM suggested inputs for Dl, Twi, and Da in activation of *sna* gene expression (Ip et al., 1992c; Kosman et al., 1991; Leptin, 1991). Hückebein (Hkb) repressor has been shown to refine the posterior border of *sna*, but plays no role in regulating its expression in the trunk region (Reuter and Leptin, 1994). Two CRMs regulate *sna* in the early embryo (Dunipace et al., 2011; Perry et al., 2010), but only the recently characterized distally-located CRM supports expression with a clear 'on/off' (i.e. sharp) boundary similar to native *sna* pattern and is required for viability (Dunipace et al., 2011) (Figures S1A–C'). Here we report that Su(H) negatively regulates expression of the *sna* gene via its distal enhancer and also mediates repression of many other genes expressed dorsal to *sna*. Our data show that the balance between Su(H) and activators defines distinct boundaries of gene expression along the entire DV axis of the *Drosophila* embryo.

RESULTS

cis-regulatory inputs to *sna* proximal and distal CRMs differ

sna expression is compromised in *dl* or *twi* mutants (Ip et al., 1992c; Leptin, 1991). To investigate the *cis*-regulatory mechanisms supporting *sna* expression, we assayed the ability of proximal or distal *sna* CRMs to support expression in mutants. In the absence of Dl nuclear localization (i.e. *gd7* mutant background), expression of both reporters was lost as had been previously observed for endogenous *sna* (data not shown). In the absence of Twi, however, the two CRMs exhibited different behaviors; expression through the proximal CRM was supported in ventral domains of the embryo, but at reduced levels (Figures S1F,G) and was comparable to endogenous *sna* expression (data not shown). In contrast, expression of the distal CRM was lost in *twi* mutant embryos (Figures S1H,I). A recent study of two enhancers acting at the *brinker* (*brk*) locus, another gene expressed along the DV axis, suggested a role for autoregulation in supporting expression of this gene (Dunipace et al., 2013). Therefore, we also tested a role for Sna and found that it is required to support expression of the distal CRM but is dispensable for the proximal CRM (Figures S1L, M and Figures S1J, K respectively). The boundary of gene expression supported by the distal CRM is sharp whereas that of the proximal is not. Moreover, many studies in the embryo have suggested Sna functions as a transcriptional repressor (e.g. Ip et al., 1992b; Leptin, 1991). Therefore, we hypothesized that Sna supports its own expression by affecting another repressor.

The *sna* distal CRM as a handle to track dorsally-acting repressor activity

To provide insight into the identity of this putative repressor, we used a chimeric enhancer assay to test whether the CRMs that support *sna* embryonic expression are influenced by dorsally-acting repression. Chimeric enhancer assays involve placing two *cis*-regulatory sequences in tandem upstream of a reporter gene and analyzing the combined output of these sequences (Figures 1A, B). Briefly, the DNA sequence to be assayed for repression

activity is placed next to the *even-skipped* stripe 3/7 (st3) CRM, which supports expression predominantly within one stripe along the AP axis in the trunk (with a weaker second stripe of expression present at the posterior) (Small et al., 1996). Reporter expression, or rather lack thereof, at the st3 expression domain serves as a way to "track" repression activity acting through the flanking CRM sequence. Repressors associated with the tested fragment may influence reporter output either by affecting activators associated with the st3 CRM sequence (i.e. quenching/long-distance action) or the promoter (i.e. direct repression) (rev. in Payankaulam et al., 2010). A similar approach has been used previously to track repressors acting in dorsolateral regions of the embryo, which define the *ind* gene dorsal boundary (Garcia and Stathopoulos, 2011; Stathopoulos and Levine, 2005c). Using this chimeric enhancer approach, the 2kb *sna* distal CRM was assayed in tandem to st3. Reporter expression was observed in ventral regions, where *sna* is expressed, whereas expression in the st3 domain was diminished (Figure 1E, compare with Figures 1C,D). In contrast, when a fragment of the proximal CRM was assayed in a similar manner, expression was observed both in ventral regions as well as in the st3 domain; only a small gap in ventrolateral regions of the st3 domain was observed (Figure 1F).

Dorsolateral repression activity observed in chimeric enhancer assays with the *sna* distal CRM could stem (i) from a complete block of st3 activity due to insulation or other enhancer blocking mechanisms (rev. in Maeda and Karch, 2007), or (ii) because dorsally-acting factors repress st3 expression in the domain dorsal to the *sna* boundary as for the *ind* gene (e.g. Stathopoulos and Levine, 2005b). To distinguish between these possibilities, focusing on the 2kb distal CRM that exhibited a stronger phenotype, we divided this sequence into four smaller overlapping fragments and assayed each fragment's ability to support repression (Figure 1G). Only one of four fragments, *sna* distal CRM fragment II ("sna_{D}.II"), supported repression that was modulated along the DV and was able to block expression of st3 in lateral and dorsal regions, consistent with the domain expected for a repressor acting to establish the *sna* boundary (Figure 1I, compare with Figures 1H,J,K). In addition, repressors known to act at the st3 CRM, Hunchback (Hb) and Knirps (Kni), were also able to affect the *sna* CRM-supported output (i.e. expression in ventral regions) as the ventral pattern exhibited gaps in expression along the AP axis (Figure 1I, see arrowhead).

A minimal 97 bp fragment of the *sna* distal CRM receives activator and repressor inputs

As fragment sna_{D}.II was sufficient to support repression in lateral and dorsal regions (Figure 1I) and also supported an expression pattern that is robust and sharp similar to endogenous *sna* expression (Figures 3B–B''), we further analyzed this sequence to provide insight into how the *snail* pattern is regulated. To identify relevant binding sites, fragment sna_{D}.II was divided into five pieces (Figure 2A) and assayed individually in chimeric enhancer assay (see Figures 2B, D–G). Of the smaller fragments, only one fragment $sna_{D.II}$.1 (i.e. *sna* distal CRM, fragment II, section 1) supported repression of st3. This repression is seen only weakly in dorsal regions while stronger, complete repression was observed in ventrolateral regions (Figure 2B). Expression in ventral regions within the domain normally encompassed by *sna* was detected with $sna_{D.II}$.1, even when complexed with st3. In contrast, the ventral expression supported by the larger sna_{D}.II fragment was repressed along the AP axis (Figure 2B, compare with Figure 1I). These results suggest that the relevant repressors (those acting

along the AP to establish st3, Hb and Kni, as well as the putative *sna* repressor activity being tracked) are not as effective at silencing this 97 bp $sna_{D.II}$.1 fragment as compared to the 567 bp sna_{D}.II fragment. It is possible that other sites present in the larger fragment are required to support stronger repression activity.

Importantly, the 97 bp $sna_{D.II}$.1 fragment appeared to be an input for repression as well as activation and was able to drive expression of the reporter in a domain with the same dorsal boundary as the endogenous *sna* gene (Figures 2C-C”). Therefore, position weight matrices (PWMs) of transcription factor consensus binding site information (Jaspar database) were used to scan the 97 bp fragment $sna_{D.II}$.1 for relevant binding sites; one bHLH site, shown to bind Twi (Ozdemir et al., 2011), and three Su(H) sites (Morel and Schweisguth, 2000) were identified (Figure 2H). When the 97 bp fragment was divided into smaller 45 bp overlapping segments, none were sufficient to fully support expression in ventral regions or repression of st3 (Figures 2I–K). Only the middle 45bp segment ($sna_{D.II}$.1–45b), which contained the three Su(H) binding sites displayed a patchy expression in ventral regions as well as relatively weak repression of st3 (Figure 2J). Furthermore, when either Twi or Su(H) sites were mutated within the $sna_{D.II}$.1 fragment, localized expression in ventral regions was lost, suggesting synergy between these factors contributes to activation in ventral regions (Figures 2L–O; Furriols and Bray, 2001). Derepression of st3 in the ventrolateral domain was also observed upon mutation of either sites, particularly following loss of Su(H) sites (Figures 2M,O compare with Figure 2B). In addition, when Su(H) binding sites were mutated, general expression throughout the embryo trunk was observed extending as far as dorsal regions (Figure 2O). These results suggested that Twi and Su(H) may act together to support *sna* expression in ventral regions of the embryo.

Loss of Su(H) activity leads to expansion of the *sna* as well as *sim* expression boundaries

We investigated whether Su(H) functions as a dorsally-acting repressor to limit the *sna* expression boundary. A total of six Su(H) binding sites were identified within the 2kb distal CRM, all of which are located in the 567 bp sna_{D}.II fragment (Figure 3A), and this is also the only portion of the 2kb distal CRM that exhibited dorsal repression activity (see Figure 1I, compare with Figures 1H,J,K). This fragment also supported a robust and sharp expression pattern similar to the 2kb CRM, almost identical to endogenous *sna* pattern observed in the ventral regions (Figures 3B–B’’). Upon mutation of Su(H) sites (Figure 3C), the 567 bp sna_{D}.II *Su(H)*Δ fragment supported reporter expression that was no longer sharp and extended beyond the endogenous *sna* expression domain by 1–2 cells (Figures 3D–D”, compare with Figures 3B–B”). This expansion corresponds to the domain of expression for the transcription factor Twi which normally extends ∼1–2 cells beyond the *sna* expression boundary (Figures 4C’’, 4D’’). Thus, the degree of expansion observed upon mutation of Su(H) binding sites is in line with what would be expected of a Twi-dependent response freed from Su(H) mediated repression. In addition, when Su(H) sites were mutated in the sna_{D}.II fragment in chimeric enhancer assay with st3, st3 expression was recovered in dorsolateral regions (Figures 3E–E”, compare with Figure 1I). These results suggest that Su(H) corresponds to the repressor activity that had been tracked by the chimeric enhancer assay.

To test the role of Su(H) in supporting *sna* expression, mutant embryo phenotypes were examined. As *Su(H)* transcripts are deposited maternally and the mutant is zygotic lethal, embryos were obtained from germline clone females (Morel and Schweisguth, 2000). *sim* exhibits a variable phenotype in these mutant embryos: gaps in the single-line of expression are observed along the AP axis, whereas in other positions the pattern is expanded from the normal pattern of one cell in width to encompassing three or more cells (Figure 4B', compare with Figure 4A') (Morel and Schweisguth, 2000; data not shown). *sna* expression in mutant embryos was also abnormal; the boundary appeared 'non-sharp' and jagged (Figure 4B, compare with Figure 4A). This phenotype may relate to the gaps observed in the *sim* expression domain, as Sna is known to repress *sim* expression, and where *sna* was expanded appears to correlate with these gaps in the *sim* pattern (Figure 4B", compare with Figure 4A"). These results support the view that (i) Su(H) is required to define the *sna* boundary as well as the dorsal boundary of *sim* and (ii) loss of *sim* expression observed in *Su(H)* mutant embryo may result, at least in part, from expansion of the *sna* expression domain.

However, our *cis*-regulatory analysis of the 97 bp $sna_{D.II}$.1 fragment also suggested a role for Su(H) in weakly supporting activation of this reporter in ventral regions (Figure 2J). Notch signaling has been shown to bias Su(H) toward activation; previous studies have demonstrated a role for this pathway, specifically, in support of *sim* expression. Therefore, we used an antibody that recognizes the Notch intracellular domain (N^{ICD}) to provide insight into the Notch signaling pathway activation profile within early embryos. N^{ICD} is cleaved from full-length protein and internalized upon signaling pathway activation (rev. in Bray, 2006). We found that N^{ICD} was present within cells in the entire ventral region of the embryo and that, in contrast, it was associated with cell surface membranes dorsal to the Twi boundary (Figures 4C-C'', 4D-D'''). As lack of N^{ICD} staining at the membranes is thought to correlate with activation of Notch signaling, this result suggests that Notch is active broadly in ventral regions of the embryo (Couturier et al., 2012). However, as the Notch ligand Delta is also internalized in ventral regions (De Renzis et al., 2006), it is possible that low levels activity may result in this domain due to *cis*-inhibition of the receptor (rev. in del Alamo et al., 2011). In contrast, more dorsally where levels of the Delta ligand for Notch transition from low to high, trans-activation of the Notch receptor by high Delta in flanking cells may support a peak of Notch signaling that helps to turn on *sim* (Figures 4C–C'', F,G).

Collectively, chimeric enhancer analysis as well as N^{ICD} stainings, support the view that in the ventral regions Su(H) is a weak activator, whereas dorsal to the *sim* domain Su(H) functions as a dedicated repressor. To test the idea that Su(H) functions as a dedicated repressor in dorsal regions of the embryo, we examined if it impacts positioning of other gene boundaries that are expressed in ventrolateral and dorsal domains along the DV axis.

Mutant phenotypes and ChIP-seq analysis identify a general DV patterning role for Su(H)

The expression of genes *sog*, *vn*, *brk*, *rho*, and *ind* was examined in embryos obtained from *Su(H)* germline clone females. Dorsal expansion of the expression domain was observed for all genes examined (Figures 5H–L compare with Figures 5C–G). The phenotypes associated with genes *sog*, *brk*, and *vn* were clearly distinguishable when compared to wildtype

embryos (Figures 5H,I,L, compare with Figures 5C, D, G). The phenotypes exhibited by *ind* and *rho* genes were more subtle and yet reproducible: the *ind* expression domain is expanded by 1–2 cell widths into dorsal regions (Figure 5J, compare with Figure 5E), whereas the effect on *rho* presents as upregulation within the interstripe domain (Figures 5K, compare with Figure 5F).

To provide further evidence that Su(H) regulates expression of these genes via binding to their respective CRMs, we performed chromatin immunoprecipitation followed by high-throughput sequencing (ChIP-seq) (Johnson et al., 2007). Strong occupancy was observed at the DNA sequence corresponding to sna_{Distal} (see above) and the previously characterized *sim* CRMs (Morel and Schweisguth, 2000) providing evidence for a direct role for Su(H) in regulating expression of these genes (Figures 5A, B). When the entire *Drosophila* genome was examined, Su(H) occupancy was also found to be associated with many previously characterized CRMs for genes expressed along the DV axis including *sog*, *brk* and *vn* (Figures 5M, Q, U) in addition to *sna* and *sim*.

As Su(H) binding to these CRMs was suggested by the ChIP-seq analysis and Su(H) binding sites are also present in these sequences, we decided to assay previously characterized CRMs for sog_{Distal}, *brk*5’ and *brk*3’ in chimeric enhancer assay with st3. The chimeric enhancer assay provided evidence that dorsally-localized repression was also associated with these *cis*-regulatory elements (Figures S2A–K; data not shown). Subsequently, we mutated the Su(H) binding sites within some of the respective CRMs for genes that showed dorsal expansion phenotypes within *Su(H)* mutant embryos as well as Su(H) occupancy by ChIP-seq. These enhancers support expression in either ventrolateral (i.e. *brk*, and *vn*) or broad lateral (i.e. *sog*) domains. Su(H) binding sites were identified in the sog_{Distal}, *brk*5’, *brk*3’, and *vn* CRMs but not in the sog_{Proximal} CRM (see Supplemental Table S1). Furthermore, Su(H) and Dl binding sites can overlap, and in several cases such overlapping sites were identified within these CRMs (Figures 5 N,R,V). Dl, Twi, and Su(H) linked binding sites have been classified as a regulatory motif called the neurogenic ectoderm enhancer signature; the idea being that close linkage of sites can better support activation in domains where the levels of Dl and Twi change significantly (for instance in ventrolateral regions of the embryo) (Crocker et al., 2008; Erives and Levine, 2004). Therefore, we mutated the Su(H) binding sites within specific CRMs, taking care not to affect any bases overlapping with Dl binding sites.

When the two Su(H) sites were mutated in the *vn* CRM, the pattern was expanded resulting in patchy, ectopic expression of the reporter in dorsal regions (Figure 5X, compare with Figure 5W). While, when the two Su(H) sites linked to Dl sites were mutated in the *brk*5’ CRM, expression was supported in a broader domain and at a later stage than the native *brk*5’CRM (Figure 5T, compare with Figure 5S). Normally *brk*5’ CRM supports early expression in ventrolateral regions of the embryo that is extinguished at cellularization, at which point *brk* gene expression is instead driven by another CRM (i.e. *brk*3’ CRM; Dunipace et al., 2013). Surprisingly, when the three Su(H) binding sites within the sog_{Distal}.III CRM were mutated, the pattern was expanded such that instead of a lateral domain of expression, the signal throughout the embryo became ubiquitous and weak (Figure 5P, compare with Figure 5O). Both dorsal as well as ventral derepression was

observed. The dorsal expansion is consistent with our model that Su(H) mediated repression is acting in dorsal regions; however, the ventral expansion observed suggests that mutagenesis of these particular Su(H) binding sites might also affect the action of other factors. In general, mutation of Su(H) binding sites supported expansion of the expression domain as would be expected by loss of a repressor; a result consistent with the phenotype of embryos from *Su(H)* germline clones and occupancy of Su(H) at these CRMs demonstrated by the ChIP-seq analysis (see Figure 5).

Combinatorial regulation between Su(H) and activators Dl and Zld control positioning of dorsal gene boundaries along the DV axis

To test whether combinatorial regulation might influence positioning of expression boundaries, we constructed a series of synthetic enhancer constructs and examined how combinations of transcription factor binding sites may relate to support of gene expression along the DV axis. As the backbone synthetic enhancer, we used a 45 bp element containing two Dl binding sites present in the *sog* distal CRM (Figure 5N). This 45 bp element was assayed in a chimeric enhancer assay with st3 to test for evidence of repression along the DV axis; furthermore, the st3 pattern also served as internal control to ensure that staining conditions were roughly equivalent. For multiplex in situ hybridization experiments, the *ind* gene expressed in dorsolateral regions of the embryo was used as a DV axis reference point by which to measure changes in border positioning in the various synthetic constructs (Figure 6; see also Figures S3A–J).

When a Su(H) binding site was added proximal to two Dl binding sites, 2x*Dl*-free*Su(H)*, the supported pattern refined from a weak ubiquitous expression domain that expanded several cells above *ind* domain (Figure 6A), to a pattern exhibiting more localized expression in ventrolateral regions, overlapping with *ind* expression (Figure 6B). Upon addition of one additional Su(H) binding site, however, synthetic enhancer expression was restricted more to the ventral regions and it no longer showed overlap with *ind* expression domain (Figure 6C). These results suggest that Su(H) can promote repression in the context of the flanking Dl sites as the addition of one or more Su(H) sites change the domain and level of expression along dorsolateral regions. However, no repressive effect was observed on st3 (for any of these chimeric enhancer constructs tested) which may relate to a requirement of other sequences to support long-range repression.

As Dl and Su(H) binding sites can overlap (e.g. see sog_D.III and *brk*5’ CRMs; Figures 5N,R), we investigated the effect of overlapping sites on synthetic reporter expression. When the two Dl-Su(H) overlapping sites were assayed, little to no expression was supported along the DV axis (Figure 6E). When these sequences were organized in tandem, expression in ventral regions was supported (Figure 6C). In contrast, when only one of the two Su(H) binding sites was designed to overlap with the Dl site, expression in ventral regions was retained (Figure 6D). Surprisingly, this construct also supported a sharp boundary (Figure 6D, and Figures S3K,K’).

This observation may relate to the Notch signaling acting as a molecular switch to support action of Su(H) as “Janus” factor: activator in ventral regions opposed to repressor in lateral and dorsal regions. Our data suggest that low levels of Su(H) complexed to N^{ICD} present in

ventral regions synergize with Dl to support activation; but where Notch is not active, Su(H)'s role as activator is no longer supported and Su(H)-mediated repression dominates. Furthermore, cooperative interactions between activators help define the extent of expression. For instance, the sharp boundary of expression supported by Dl and Su(H) sites in this synthetic construct correlates with the position of endogenous *sim* expression (Figures S3K,K'); while, in contrast, the 97 bp minimal *sna* enhancer containing Twi and Su(H) sites supported expression just one cell ventral to *sim*, correlating instead with the endogenous *sna* boundary (Figure 2C"). The Twist gradient is steeper than that of Dl. These findings highlight the difference between activators Dl and Twi and suggest that how they interact with Su(H) can position distinct gene expression boundaries along the DV axis.

We found that adding a Zld binding site to the 2x*Dl* synthetic construct did not change the expression output (Figure 6F, compare with Figure 6A). Previous studies have suggested that Zld can expand the activation potential of Dl (Liberman and Stathopoulos, 2009). However, here the synthetic constructs were assayed as chimeric enhancers that incorporate a flanking st3 sequence; in this case, broad expression output supported by the *2xDl* synthetic reporter may represent the maximum Dl-dependent output. The st3 sequence contains binding sites for Zld (Struffi et al., 2011) and/or other factors that help Dl to support expression in a broad domain. In any case, we investigated whether Su(H)-repression could counteract activation supported by closely positioned Dl-Zld sites.

When a Su(H) binding site was introduced to the 2x*Dl-Zld* synthetic as an overlapping site with of one of the Dl sites, the boundary of expression was shifted ventrally (Figure 6G). Converting both of the Dl binding sites to overlapping Dl-Su(H) sites weakened expression further ventrally (Figure 6H, compare with Figure 6G). Interestingly, however, both *Dl*-[*Dl-Su(H)*]-*Zld* and 2x[*Dl-Su(H)*]-*Zld* synthetics supported expression that were more robust and stronger in the ventral regions than the non-Zld containing versions, *Dl*-[*Dl-Su(H)*]-*Su(H)* and 2x[*Dl-Su(H)*] (Figures 6G,H compare with Figures 6C,E). These results are consistent with a role for Su(H) as repressor and Zld as activator to counterbalance repression, and show that Su(H) can compete against activator(s) even those such as Zld which function in broad domains.

We also tested whether organization of binding sites within the synthetic enhancers can impact the expression outputs. When a Zld binding site was introduced between two Dl sites in a synthetic construct as found in the sog_{Distal}CRM (sog_{Distal}.III; Figure 5N), the pattern supported was broad and lateral (Figure 6I compare with Figure 6F) contrasting with the ventral pattern supported by other constructs in which Zld was positioned downstream of the Dl sites (Figure 6F,G,H). However, when a Su(H) binding site was introduced into the *Dl-Zld-Dl* synthetic such that the second Dl site was overlapping with Su(H), similar to previous results (Figures 6B–E,G, and H), expression along the DV axis was greatly reduced (Figure 6J).

To test whether repression caused by Su(H) binding sites was direct, we checked the expression of the *Dl*-[*Dl-Su(H)*]-*Su(H)*, and 2x*Dl*-2xfree*Su(H)* synthetics in embryos from *Su(H)* germline clone females. In the mutant embryos, expression supported by either synthetic was no longer restricted to the ventral domains, but expanded to dorsal regions of

the embryo (Figures 6K, L compare with Figures 6C,D), similar to the pattern supported by the 2x*Dl* synthetic construct that only contains Dl binding sites (Figure 6A).

Overall, these experiments support the view that Su(H) can act as a repressor to affect patterning along the DV axis and that gene expression outputs result from a balance of interactions between activators and repressors. The combination of factors present as well as the number and organization of their binding sites can strongly influence the position of boundaries (Figure 6M).

Ectopic expression of N^{ICD} results in expansion of the dorsal boundaries for many DV genes

Previous studies from other developmental contexts, namely bristle formation, have shown that activation of Notch can bias Su(H) toward activator form rather than repressor (e.g. Castro et al., 2005). Therefore, we simulated the active Notch environment by expressing N^{ICD} ectopically using a UAS-*N*^{ICD} construct driven by *nosGal4-GCN-bcd*3'UTR to tip the balance from Su(H) as repressor towards Su(H) as activator at the anterior of embryos. Ectopic expression of DV genes was observed at the anterior half of the embryo, whereas the posterior half served as negative control (Figure 7I). Upon N^{ICD} induction, the *sim* expression domain was expanded dorsolaterally to a region of 5–6 cells at the anterior end of the embryo (Figure 7B, compare with Figure 7A). This domain likely corresponds to where Dl and possibly Su(H) complexed with N^{ICD} are competent to support activation. In turn, *sna* was expanded by 1–2 cells to the domain where Twi and Su(H)-N^{ICD} are likely competent to support gene expression; furthermore, the *sna* boundary was no longer sharp but jagged (Figure 7H, compare with Figure 7G). Surprisingly, weak ectopic expression of *sna* was also observed in dorsolateral regions; suggesting that N^{ICD}, complexed with Su(H) can, albeit weakly, support *sna* expression. Similar to *sim* and *sna*, *sog* and *vn* also showed dorsally expanded expression patterns at the anterior half of the embryo upon ectopic N^{ICD} expression (Figures 7D,F compare with Figures C,E). The expanded expression observed in more dorsal regions likely results from activation gained as a result of N^{ICD} functioning in a permissive (i.e., 'anti-repressive) rather than instructive role (see Discussion; Tapanes-Castillo and Baylies, 2004).

DISCUSSION

We have identified an important role for Su(H) in defining borders of genes expressed along the DV axis in the *Drosophila* early embryo. Identification of Su(H) as a broadly acting repressor to support DV patterning helps explain how boundaries specified along this axis can be differentially positioned even in domains where the Dl gradient is shallow (Reeves et al, 2012). This study highlights that Su(H) helps to establish many different boundaries of expression, and that the balance between activators as well as repressors differentially positions gene expression boundaries across the entire *Drosophila* DV axis.

Previous studies have suggested that Notch signaling can act as a molecular toggle to switch Su(H) activity from a repressor to an activator (rev. in del Alamo et al., 2011) and that Su(H) can act as an activator in the sea urchin embryo within a broad embryonic domain (Ransick and Davidson, 2006). Nevertheless, a broader role for Su(H) in supporting

patterning along the entire DV axis of the *Drosophila* embryo, beyond regulation of *sim*, has not been appreciated. We propose that Notch signaling is active in the entire ventral domain of the embryo and inactive dorsal to the Twi expression domain (Figures 4C–G). At the interface, where Twi levels sharply decrease, Su(H) activity also changes. Su(H)'s role as activator may peak, possibly due to lateral induction of Notch signaling by the Delta ligand, and thereby aid in supporting *sim* expression, which also receives input from the Dl transcription factor. Alternatively, in the ventral-most regions, although Su(H) is required to support high levels of *sna* expression, it is not sufficient to support its expression (Figure 2J). This likely relates to the fact that *sna* expression is also dependent on Twi (e.g. see Figures 2B,M,O, and Figures S1H,I) and that ectopic N^{ICD} expression only induces weak *sna* expression in dorsolateral domains (Figure 7H). Notch signaling may help sharpen the *sna* and *sim* boundaries, because it influences the domains where Su(H) acts as an activator (Figures 4F, and 4G).

The specific differential positioning between *sna* and *sim* (by a difference of one cell) may relate to different inputs into the respective CRMs either through different sets of activators, number and/or quality of binding sites. Our data support the view that Twi and Su(H) define the *sna* dorsal boundary, with both factors acting synergistically to support activation in ventral regions and Su(H) acting as a repressor in lateral/dorsal regions to define the boundary position. We suggest that additional inputs by Dl and Zld into the *sim* gene are responsible for allowing the boundary of this gene to extend one-cell width farther than that of *sna*. *sim* expression is also repressed ventrally by Sna (e.g. Cowden and Levine, 2002). These results are supported by our synthetic enhancer analysis because combination of Twi +Su(H) sites versus Dl+Su(H) sites promotes sharp boundaries that differ by one cell; the former overlaps with *sna* and the latter with *sim* (data not shown and Figure 6D, Figures S3K,K'). Previous studies have also suggested that Notch signaling per se is not required to support *sim* expression through transcriptional activation but to support 'anti-repression' (Morel and Schweisguth, 2000). In particular, it was shown that a *sim* reporter construct in which Su(H) binding sites were mutated was able to support gene expression even in *Notch* germline clone embryos; this results supports the view that Notch signaling is required to promote *sim* expression through an anti-repression mechanism, where it allows activators to compete against Su(H) mediated repression (see also Tapanes-Castillo and Baylies, 2004).

Furthermore, Sna has been previously shown to support Notch signaling pathway activation in the early embryo. Sna-mediated repression of the Bearded family proteins allows the E3 ubiquitin ligase Neuralized (Neur) to be active in the ventral regions of the embryo. Neur is required for endocytosis and activity of Notch ligand, Delta (Bardin and Schweisguth, 2006; De Renzis et al., 2006). Therefore, positive feedback between Sna and Notch signaling may ensure that the *sna* boundary is sharp wherever it is positioned. Furthermore, our *cis*-regulatory analysis demonstrates a role for Sna in supporting its own expression. This autoregulation of *sna* expression may work through indirect regulation of Notch signaling; alternatively Sna may influence which of its CRMs is able to engage with its promoter (e.g. see Dunipace et al., 2013). For instance, the role of the Dl-dependent and Twi-independent proximal CRM (see Figures S1F,G) may simply be to support early *sna* expression until Twi levels are high enough to support expression through the distal CRM. Multiple feedback

mechanisms, also including other dorsally-acting repressors yet to be identified, likely act to ensure the proper positioning of *sna* expression domain that establishes the mesoderm-mesectoderm-neurogenic ectoderm boundaries.

Some genes along the DV axis receive input from repressors other than Su(H), and one such example is the gene *ind* (Figure 7J). Evidence for dorsally-acting repression on *ind* was obtained from both CRM analysis and genetic experiments, which suggested that the repressor Capicua (Cic) might support dorsal repression through a 12bp A-box element (Ajuria et al., 2011; Garcia and Stathopoulos, 2011; Stathopoulos and Levine, 2005c). However, Cic's influence seems to be limited to *ind*, as other genes expressed along the DV axis do not exhibit dorsally expanded expression domains in *cic* mutants nor do their CRMs contain matches to the A-box/Cic consensus sequence (M.Garcia and A.S., unpub. obs.). Besides Cic, the Schnurri-Mad-Medea (SMM) complex, a repressive complex activated by TGF-β signaling, has been linked to repression of *ind* as well as *vnd* dorsal boundaries (Crocker and Erives, 2013; Garcia and Stathopoulos, 2011; Mizutani et al., 2006). The SMM complex recognizes a 16 bp binding consensus but besides *ind* and *vnd* CRMs, only the *sog* promoter-proximal CRM contains a sequence match to this consensus (Supplemental Table S1). We suggest that the SMM- and Cic-mediated repression constrains the position of expression domains for the genes they influence (i.e. support hard boundaries), perhaps, because the repressors are themselves spatially localized (see Garcia et al., 2013). Similar mechanisms using multiple, spatially defined repressors to establish 'hard' boundaries have been uncovered in other patterning systems: patterning of the anterior domain of the AP axis of *Drosophila* embryos and the neural tube specification in vertebrates (Balaskas et al., 2012; Chen et al., 2012; Lohr et al., 2009; Oosterveen et al., 2012). In contrast, the data presented here supports the view that the Su(H) acts to counterbalance Dl and Zld mediated activation in a broad domain, affecting many genes expressed along the DV axis.

Our results suggest that positioning of genes along the DV axis is first directed by an approximation, a "pre-pattern" formation defined by gradients of activators and binding site specificity. This pre-pattern is refined by the action of repressors acting both dorsally and ventrally to establish final positioning of genes with a range of boundary positions (Figure 6K). Input by broadly-acting factors like Zld or Su(H) may ensure that patterns initiated by graded activators (e.g., Dl, Twi) have flexible domains of expression that span the entire DV axis.

EXPERIMENTAL PROCEDURES

Drosophila strains and genetic crosses

Flies were reared in standard cornmeal food at 25°C unless otherwise indicated. The genotype *yw* was used as wild-type. *Adh^{n7}sna^{1}cn^{1}vg^{1}/CyO* (Bloomington 25127) and *twi^{1}b^{1}pr^{1}cn^{1}bw^{1}/CyO* (Bloomington 6147*)* fly stocks were rebalanced with *CyO ftz-lacZ* or *CyO Hb-lacZ* marked balancers, respectively. The CRM containing the 6 kb *sna*$_{\text{Proximal}}$-*lacZ* reporter have been published previously (Ip et al., 1992c). *Su(H)* $^{\Delta 47}$ is a null allele (Morel and Schweisguth, 2000); *Su(H)*$^{\Delta 47}$ FRT40A P[*l(2)35Bg* $^{+}$]/*CyO* was used to make germline clones (a gift from S. Artavanis-Tsakonas; Harvard, USA). UAS-N^{ICD} (Struhl and Greenwald, 2001) and *nos*Gal4-*GCN-bcd*3'UTR (Janody et al., 2000) were gifts from Terry

Orr-Weaver (MIT, USA) and Heinrich Reichert (Biozentrum, University Basel, Switzerland), respectively. A 25 kB *sna-GFP* rescue construct was used and described previously (Dunipace et al., 2011).

We used the FLP-FRT system to generate $Su(H)^{\Delta 47}$ germline clones (Chou and Perrimon, 1996) as described previously (Morel and Schweisguth, 2000). In brief, *hs-FLP1*; *Sco/CyO* virgin females (Bloomington stock 1929) were crossed with ovo^{D1} FRT40A/*Cyo* males (Bloomington stock 2121). Non-*Sco*, *Cyo* F_1 males were crossed with $Su(H)^{\Delta 47}$ FRT40A P[*l(2)35Bg* $^+$]/*CyO* virgin females. Second- to third-instar F_2 larvae were heat shocked 2 times for 1 hour per day at 37°C in a waterbath. Embryos were collected from *non-CyO* F_2 virgin females crossed to $Su(H)^{\Delta 47}$ FRT40A P[*l(2)35Bg* $^+$]/*CyO Hb-lacZ* males.

N^{ICD} ectopic expression experiments were conducted at 29°C to increase efficiency of Gal4 expression and compared with driver alone, treated equivalently.

Cloning and generation of reporter and chimeric constructs

$eve_{promoter}$-*lacZ*-attB vector (Liberman and Stathopoulos, 2009) was used as a backbone in reporter and chimeric enhancer assays. A detailed description of how reporters were constructed including a list of primers used is provided within the Supplemental Information.

Chromatin preparation, DNA isolation, amplification, and sequencing

Chromatin was prepared as described previously (Ozdemir et al., 2011) and DNA sequencing of samples was performed according to standard Illumina protocols at Caltech Genome Center. See Supplemental Experimental Procedures for additional information.

Whole-mount *in-situ* hybridization, immunological methods, and antibodies

Standard protocols were used for embryo collection, fixing and staining. Samples were collected, stained, and processed in parallel and confocal microscope images were taken under the same settings to prevent variability between samples. Embryos were hybridized with antisense RNA probes labeled with digoxigenin, biotin or FITC-UTP to detect reporter or in vivo gene expression (Bischof et al., 2007). Immunostaining was performed according to standard procedures using anti-N^{ICD} antibody (Developmental Studies Hybridoma Bank, #C17.9C6, 1:20 dilution), anti-GFP antibody (Life Technologies, #1356608, 1:500), and anti-Twi antibody (rat) raised for this study (1:100). Secondary antibodies were purchased from Molecular Probes: Anti-Mouse 555 (#A31570, 1:1000), Anti-Rabbit 488 (#A21206, 1:1000), and Anti-Rat 647 (#A21472, 1:1000).

Supplementary Material

Refer to Web version on PubMed Central for supplementary material.

Acknowledgments

We thank Spiros Artavanis-Tsakonas, Terry Orr-Weaver, Heinrich Reichert, Francois Schweisguth, Bloomington Stock Center, and Developmental Studies Hybridoma Bank for providing fly stocks and antibodies. We thank Leslie Dunipace for sharing unpublished results, Igor Antoshechkin of the Caltech Jacobs Genome Facility for

ChIP-seq library preparation and sequencing, Henry Amrheim for help with database display and managing the lab web browser, Marianne Bronner and members of the Stathopoulos lab for comments on the manuscript, and Eric Davidson for helpful discussions. This study was supported by NIH research grant R01GM077668 to A.S.

REFERENCES

Ajuria L, Nieva C, Winkler C, Kuo D, Samper N, Andreu MJ, Helman A, Gonzalez-Crespo S, Paroush Z, Courey AJ, et al. Capicua DNA-binding sites are general response elements for RTK signaling in Drosophila. Development (Cambridge, England). 2011; 138:915–924.

Balaskas N, Ribeiro A, Panovska J, Dessaud E, Sasai N, Page KM, Briscoe J, Ribes V. Gene regulatory logic for reading the Sonic Hedgehog signaling gradient in the vertebrate neural tube. Cell. 2012; 148:273–284. [PubMed: 22265416]

Bardin AJ, Schweisguth F. Bearded family members inhibit Neuralized-mediated endocytosis and signaling activity of Delta in Drosophila. Developmental cell. 2006; 10:245–255. [PubMed: 16459303]

Bischof J, Maeda RK, Hediger M, Karch F, Basler K. An optimized transgenesis system for Drosophila using germ-line-specific {varphi}C31 integrases. Proceedings of the National Academy of Sciences. 2007; 104:3312.

Bray SJ. Notch signalling: a simple pathway becomes complex. Nat Rev Mol Cell Biol. 2006; 7:678–689. [PubMed: 16921404]

Castro B, Barolo S, Bailey AM, Posakony JW. Lateral inhibition in proneural clusters: cis-regulatory logic and default repression by Suppressor of Hairless. Development (Cambridge, England). 2005; 132:3333–3344.

Chen H, Xu Z, Mei C, Yu D, Small S. A system of repressor gradients spatially organizes the boundaries of Bicoid-dependent target genes. Cell. 2012; 149:618–629. [PubMed: 22541432]

Chou TB, Perrimon N. The autosomal FLP-DFS technique for generating germline mosaics in Drosophila melanogaster. Genetics. 1996; 144:1673–1679. [PubMed: 8978054]

Couturier L, Vodovar N, Schweisguth F. Endocytosis by Numb breaks Notch symmetry at cytokinesis. Nat Cell Biol. 2012; 14:131–139. [PubMed: 22267085]

Cowden J, Levine M. The Snail repressor positions Notch signaling in the Drosophila embryo. Development (Cambridge, England). 2002; 129:1785–1793.

Cowden J, Levine M. Ventral dominance governs sequential patterns of gene expression across the dorsal-ventral axis of the neuroectoderm in the Drosophila embryo. Dev Biol. 2003; 262:335–349. [PubMed: 14550796]

Crocker J, Erives A. A Schnurri/Mad/Medea complex attenuates the dorsal-twist gradient readout at vnd. Developmental biology. 2013; 378:64–72. [PubMed: 23499655]

Crocker J, Tamori Y, Erives A. Evolution acts on enhancer organization to fine-tune gradient threshold readouts. PLoS Biol. 2008; 6:e263. [PubMed: 18986212]

De Renzis S, Yu J, Zinzen R, Wieschaus E. Dorsal-ventral pattern of Delta trafficking is established by a Snail-Tom-Neuralized pathway. Developmental cell. 2006; 10:257–264. [PubMed: 16459304]

del Alamo D, Rouault H, Schweisguth F. Mechanism and significance of cis-inhibition in Notch signalling. Curr Biol. 2011; 21:R40–R47. [PubMed: 21215938]

Dunipace L, Ozdemir A, Stathopoulos A. Complex interactions between cis-regulatory modules in native conformation are critical for Drosophila snail expression. Development (Cambridge, England). 2011; 138:4075–4084.

Dunipace L, Saunders A, Ashe HL, Stathopoulos A. Autoregulatory feedback controls sequential action of cis-regulatory modules at the brinker locus. Dev Cell. 2013; 26:536–543. [PubMed: 24044892]

Erives A, Levine M. Coordinate enhancers share common organizational features in the Drosophila genome. Proc Natl Acad Sci U S A. 2004; 101:3851–3856. [PubMed: 15026577]

Furriols M, Bray S. A model Notch response element detects Suppressor of Hairless-dependent molecular switch. Curr Biol. 2001; 11:60–64. [PubMed: 11166182]

Garcia M, Stathopoulos A. Lateral gene expression in Drosophila early embryos is supported by Grainyhead-mediated activation and tiers of dorsally-localized repression. PLoS One. 2011; 6:e29172. [PubMed: 22216201]

Gonzalez-Crespo S, Levine M. Interactions between dorsal and helix-loop-helix proteins initiate the differentiation of the embryonic mesoderm and neuroectoderm in Drosophila. Genes Dev. 1993; 7:1703–1713. [PubMed: 8370521]

Hong JW, Hendrix DA, Papatsenko D, Levine MS. How the Dorsal gradient works: insights from postgenome technologies. Proceedings of the National Academy of Sciences of the United States of America. 2008; 105:20072–20076. [PubMed: 19104040]

Huang AM, Rusch J, Levine M. An anteroposterior Dorsal gradient in the Drosophila embryo. Genes & Development. 1997; 11:1963–1973. [PubMed: 9271119]

Ip YT, Park RE, Kosman D, Bier E, Levine M. The dorsal gradient morphogen regulates stripes of rhomboid expression in the presumptive neuroectoderm of the *Drosophila* embryo. Genes & Dev. 1992a; 6:1728–1739. [PubMed: 1325394]

Ip YT, Park RE, Kosman D, Bier E, Levine M. The dorsal gradient morphogen regulates stripes of rhomboid expression in the presumptive neuroectoderm of the Drosophila embryo. Genes Dev. 1992b; 6:1728–1739. [PubMed: 1325394]

Ip YT, Park RE, Kosman D, Yazdanbakhsh K, Levine M. dorsal-twist interactions establish snail expression in the presumptive mesoderm of the Drosophila embryo. Genes Dev. 1992c; 6:1518–1530. [PubMed: 1644293]

Janody F, Reischl J, Dostatni N. Persistence of Hunchback in the terminal region of the Drosophila blastoderm embryo impairs anterior development. Development. 2000; 127:1573–1582. [PubMed: 10725234]

Jiang J, Levine M. Binding affinities and cooperative interactions with bHLH activators delimit threshold responses to the dorsal gradient morphogen. Cell. 1993; 72:741–752. [PubMed: 8453668]

Johnson DS, Mortazavi A, Myers RM, Wold B. Genome-wide mapping of in vivo protein-DNA interactions. Science. 2007; 316:1497–1502. [PubMed: 17540862]

Kasai Y, Nambu JR, Lieberman PM, Crews ST. Dorsal-ventral patterning in Drosophila: DNA binding of snail protein to the single-minded gene. Proceedings of the National Academy of Sciences of the United States of America. 1992; 89:3414–3418. [PubMed: 1533042]

Kosman D, Ip YT, Levine M, Arora K. Establishment of the mesoderm-neuroectoderm boundary in the Drosophila embryo. Science. 1991; 254:118–122. [PubMed: 1925551]

Leptin M. twist and snail as positive and negative regulators during Drosophila mesoderm development. Genes Dev. 1991; 5:1568–1576. [PubMed: 1884999]

Liang HL, Nien CY, Liu HY, Metzstein MM, Kirov N, Rushlow C. The zinc-finger protein Zelda is a key activator of the early zygotic genome in Drosophila. Nature. 2008; 456:400–403. [PubMed: 18931655]

Liberman LM, Stathopoulos A. Design flexibility in cis-regulatory control of gene expression: synthetic and comparative evidence. Developmental biology. 2009; 327:578–589. [PubMed: 19135437]

Lohr U, Chung HR, Beller M, Jackle H. Antagonistic action of Bicoid and the repressor Capicua determines the spatial limits of Drosophila head gene expression domains. Proceedings of the National Academy of Sciences of the United States of America. 2009; 106:21695–21700. [PubMed: 19959668]

Maeda RK, Karch F. Making connections: boundaries and insulators in Drosophila. Curr Opin Genet Dev. 2007; 17:394–399. [PubMed: 17904351]

Markstein M, Zinzen R, Markstein P, Yee KP, Erives A, Stathopoulos A, Levine M. A regulatory code for neurogenic gene expression in the Drosophila embryo. Development (Cambridge, England). 2004; 131:2387–2394.

Mizutani CM, Meyer N, Roelink H, Bier E. Threshold-dependent BMP-mediated repression: a model for a conserved mechanism that patterns the neuroectoderm. PLoS Biol. 2006; 4:e313. [PubMed: 16968133]

Morel V, Schweisguth F. Repression by suppressor of hairless and activation by Notch are required to define a single row of single-minded expressing cells in the Drosophila embryo. Genes Dev. 2000; 14:377–388. [PubMed: 10673509]

Moussian B, Roth S. Dorsoventral axis formation in the Drosophila embryo--shaping and transducing a morphogen gradient. Curr Biol. 2005; 15:R887–R899. [PubMed: 16271864]

Oosterveen T, Kurdija S, Alekseenko Z, Uhde CW, Bergsland M, Sandberg M, Andersson E, Dias JM, Muhr J, Ericson J. Mechanistic differences in the transcriptional interpretation of local and long-range Shh morphogen signaling. Developmental cell. 2012; 23:1006–1019. [PubMed: 23153497]

Ozdemir A, Fisher-Aylor KI, Pepke S, Samanta M, Dunipace L, McCue K, Zeng L, Ogawa N, Wold BJ, Stathopoulos A. High resolution mapping of Twist to DNA in Drosophila embryos: Efficient functional analysis and evolutionary conservation. Genome Res. 2011; 21:566–577. [PubMed: 21383317]

Payankaulam S, Li LM, Arnosti DN. Transcriptional repression: conserved and evolved features. Curr Biol. 2010; 20:R764–R771. [PubMed: 20833321]

Perry MW, Boettiger AN, Bothma JP, Levine M. Shadow enhancers foster robustness of Drosophila gastrulation. Curr Biol. 2010; 20:1562–1567. [PubMed: 20797865]

Ransick A, Davidson EH. cis-regulatory processing of Notch signaling input to the sea urchin glial cells missing gene during mesoderm specification. Developmental biology. 2006; 297:587–602. [PubMed: 16925988]

Reeves, GT.; Stathopoulos, A. Graded Dorsal and Differential Gene Regulation in the *Drosophila* Embryo. In: Briscoe, J.; Lawrence, P.; Vincent, JP., editors. Perspectives on Generation and Interpretation of Morphogen Gradients. Cold Spring Harbor Laboratory Press; 2009.

Reeves GT, Trisnadi N, Truong TV, Nahmad M, Katz S, Stathopoulos A. Dorsal-ventral gene expression in the Drosophila embryo reflects the dynamics and precision of the dorsal nuclear gradient. Developmental cell. 2012; 22:544–557. [PubMed: 22342544]

Reuter R, Leptin M. Interacting functions of snail, twist and huckebein during the early development of germ layers in Drosophila. Development (Cambridge, England). 1994; 120:1137–1150.

Rogers KW, Schier AF. Morphogen gradients: from generation to interpretation. Annu Rev Cell Dev Biol. 2011; 27:377–407. [PubMed: 21801015]

Rushlow CA, Shvartsman SY. Temporal dynamics, spatial range, and transcriptional interpretation of the Dorsal morphogen gradient. Curr Opin Genet Dev. 2012

Sarkar G, Sommer SS. The "megaprimer" method of site-directed mutagenesis. BioTechniques. 1990; 8:404–407. [PubMed: 2340178]

Small S, Blair A, Levine M. Regulation of two pair-rule stripes by a single enhancer in the Drosophila embryo. Developmental biology. 1996; 175:314–324. [PubMed: 8626035]

Stathopoulos A, Levine M. Whole-genome analysis of Drosophila gastrulation. Curr Opin Genet Dev. 2004; 14:477–484. [PubMed: 15380237]

Stathopoulos A, Levine M. Genomic regulatory networks and animal development. Dev Cell. 2005a; 9:449–462. [PubMed: 16198288]

Stathopoulos A, Levine M. Localized repressors delineate the neurogenic ectoderm in the early Drosophila embryo. Developmental biology. 2005b; 280:482–493. [PubMed: 15882587]

Stathopoulos A, Levine M. Localized repressors delineate the neurogenic ectoderm in the early Drosophila embryo. Developmental biology. 2005c; 280:482–493. [PubMed: 15882587]

Struffi P, Corado M, Kaplan L, Yu D, Rushlow C, Small S. Combinatorial activation and concentration-dependent repression of the Drosophila even skipped stripe 3+7 enhancer. Development (Cambridge, England). 2011; 138:4291–4299.

Struhl G, Greenwald I. Presenilin-mediated transmembrane cleavage is required for Notch signal transduction in Drosophila. PNAS. 2001; 98:229–234. [PubMed: 11134525]

Tapanes-Castillo A, Baylies MK. Notch signaling patterns Drosophila mesodermal segments by regulating the bHLH transcription factor twist. Development (Cambridge, England). 2004; 131:2359–2372.

Zinzen R, Senger K, Levine M, Papatsenko D. Computational Models for Neurogenic Gene Expression in the Drosophila Embryo. Current Biology. 2006; 16:1358–1365. [PubMed: 16750631]

Zinzen RP, Girardot C, Gagneur J, Braun M, Furlong EE. Combinatorial binding predicts spatio-temporal cis-regulatory activity. Nature. 2009; 462:65–70. [PubMed: 19890324]

HIGHLIGHTS

- Su(H) is a transcription factor that regulates patterning along the entire DV axis.
- Notch signaling modulates Su(H) activity spatially.
- Su(H) repression acts as a counterbalance to Dorsal- and Zelda-mediated activation.
- Synthetic enhancers provide insight into combinatorial regulation by these factors.

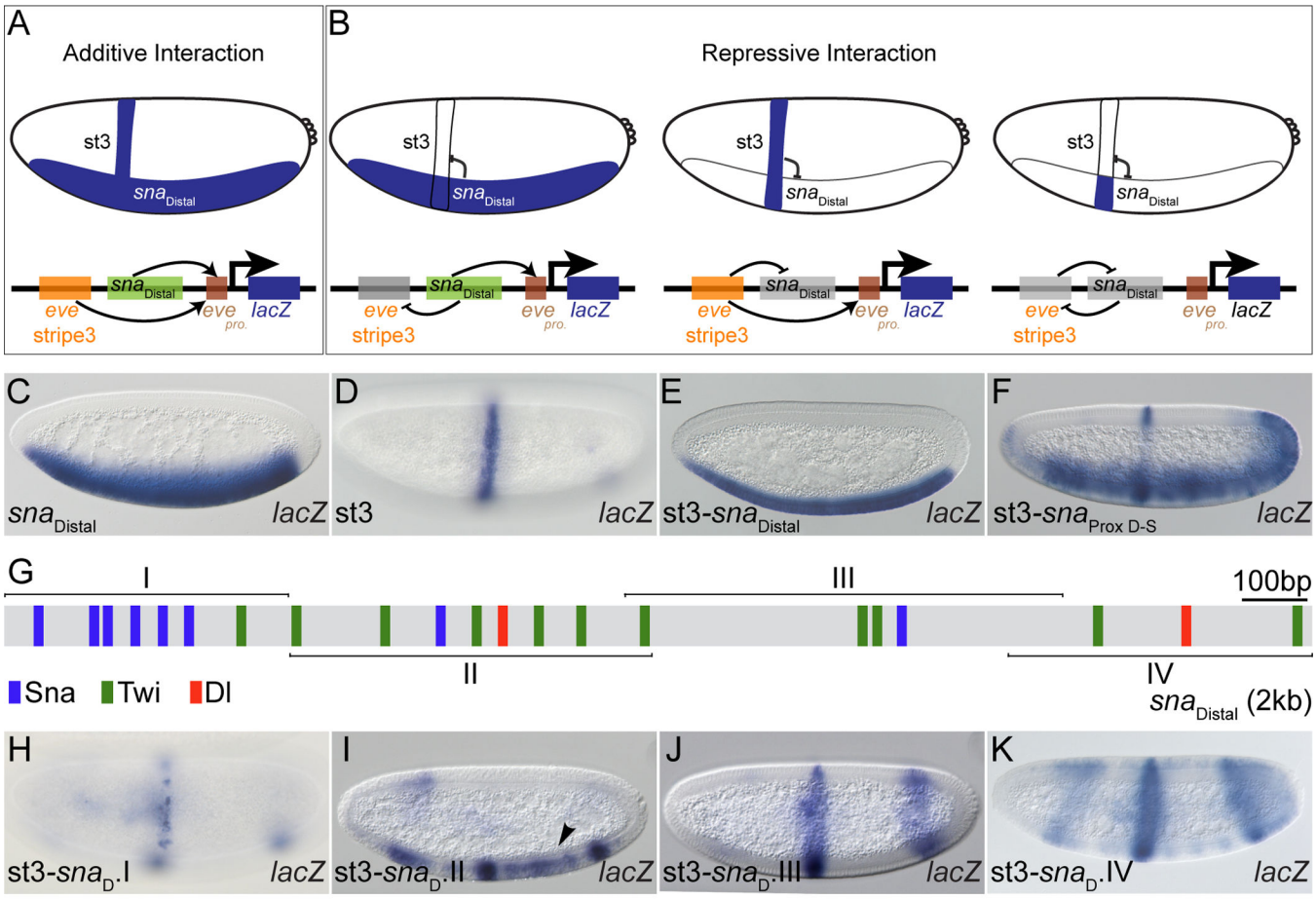

Figure 1. Tracking repression activity associated with the *sna* distal CRM using chimeric enhancer assay

(A-B) Diagrams showing summary of possible outcomes of chimeric enhancer assay between *eve-stripe 3* enhancer (st3) and the distal *sna* CRM (sna_{Distal}): additive (A) or repressive (B) interactions between CRMs are depicted.

(C-F) In this and subsequent figures, embryos are oriented with anterior to the left and dorsal up; and lateral views of embryos are shown unless otherwise noted. Embryos were assayed by in situ hybridization using riboprobes to detect *lacZ* expression supported by the sna_{Distal}, st3, chimeric st3-sna_{Distal}, and chimeric st3-$sna_{Prox\ D\text{-}S}$ reporter constructs respectively.

(G) A schematic of the 2kb sna_{Distal} CRM. Beginning and end points of four smaller sna_{Distal} fragments labeled as roman numerals I-IV (sna_{D}.I-IV) are marked by horizontal lines, and vertical boxes show position of binding sites for Sna (blue), Twi (green), and Dl (red).

(H-K) Embryos were assayed by in situ hybridization using riboprobes to detect *lacZ* expression supported by chimeric st3-sna_{D}.I-IV reporter constructs, respectively.

See also Figure S1.

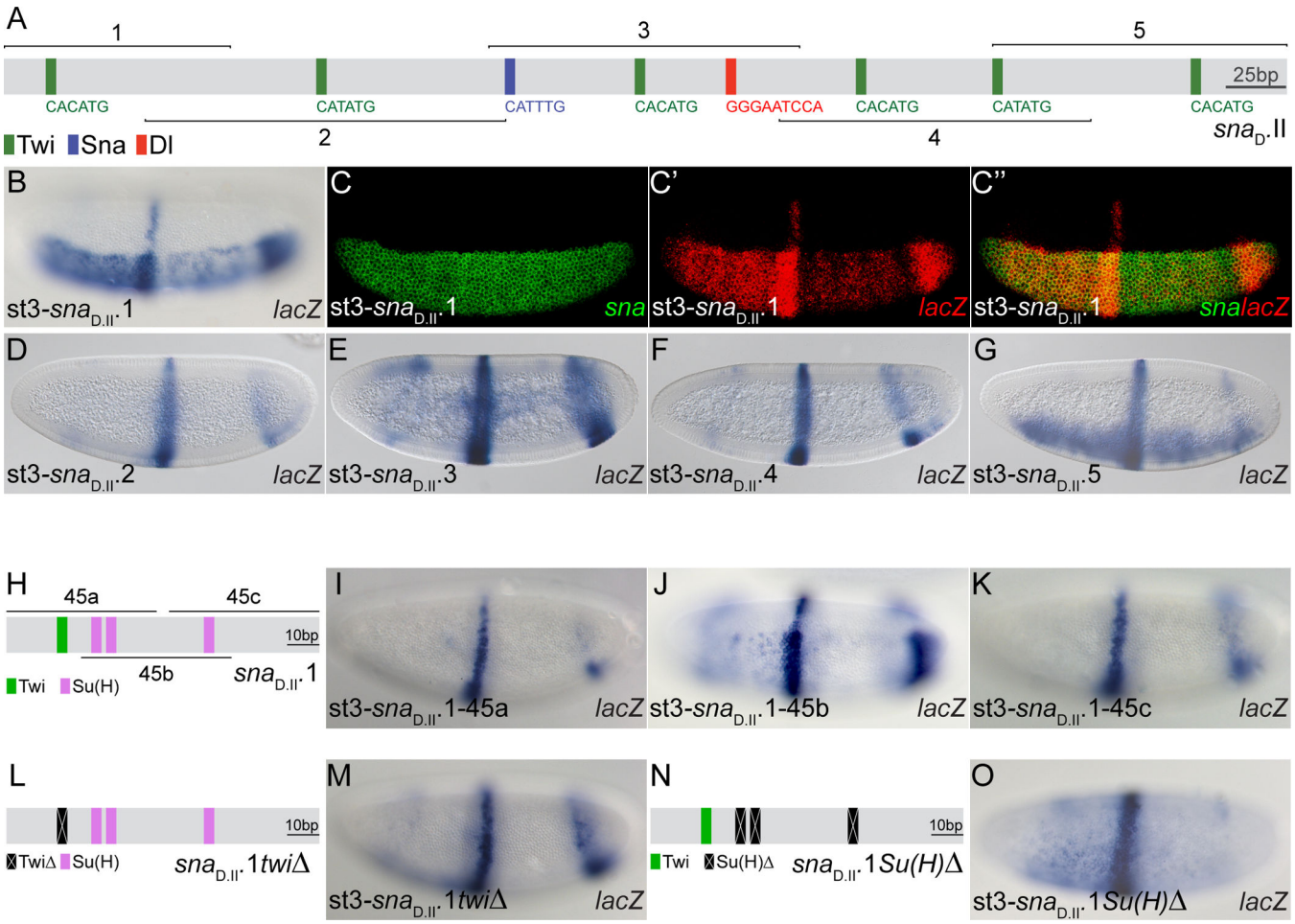

Figure 2. Su(H) binding sites within a 97bp minimal fragment support repression in chimeric enhancer assay

(A) A schematic of the 567 bp *sna*$_{D}$.II enhancer. Beginning and end points of five smaller *sna*$_{D}$.II fragments labeled as numbers 1–5 (*sna*$_{D.II}$.1–5) are marked by horizontal lines, vertical boxes showing positions of binding sites for Sna (blue), Twi (green), and Dl (red).

(B, D-G) Embryos were assayed by in situ hybridization using riboprobes to detect *lacZ* expression supported by chimeric st3-*sna*$_{D.II}$.1 - st3-*sna*$_{D.II}$.5 reporter constructs, respectively.

(C-C'') Ventrolateral view of a embryo processed by in situ hybridization using riboprobes to detect endogenous *sna* expression (green; C), and *lacZ* expression supported by chimeric *sna*$_{D.II}$.1 reporter construct (red; C'). A merge of endogenous *sna* and *lacZ* reporter expression domain is shown in panel (C'').

(H, L, N) Schematics of the intact 97bp *sna*$_{D.II}$.1 fragment (H), the version containing mutated Twi site (*sna*$_{D.II}$.1*twi*Δ; L), and the version containing mutated Su(H) sites (*sna*$_{D.II.}$1*Su(H)*Δ; N). Within panel (H), the coordinates of the three smaller *sna*$_{D.II}$.1 fragments tested (*sna*$_{D.II}$.1–45a, -b, -c) are marked by horizontal lines. Vertical boxes show positions of binding sites for Twi (green), Su(H) (magenta), and those mutated (black).

(I-K) Ventrolateral view of embryos processed by in situ hybridization using riboprobes to detect *lacZ* expression supported by chimeric st3-*sna*$_{D.II}$.1–45a, -b, and -c reporter constructs, respectively.

(M, O) Lateral view of embryos processed by in situ hybridization using riboprobes to detect *lacZ* expression supported by chimeric st3-*sna*$_{D.I}$.1*twi*Δ (M) or st3-*sna*$_{D.II}$.1*Su(H)*Δ (O) reporter constructs.

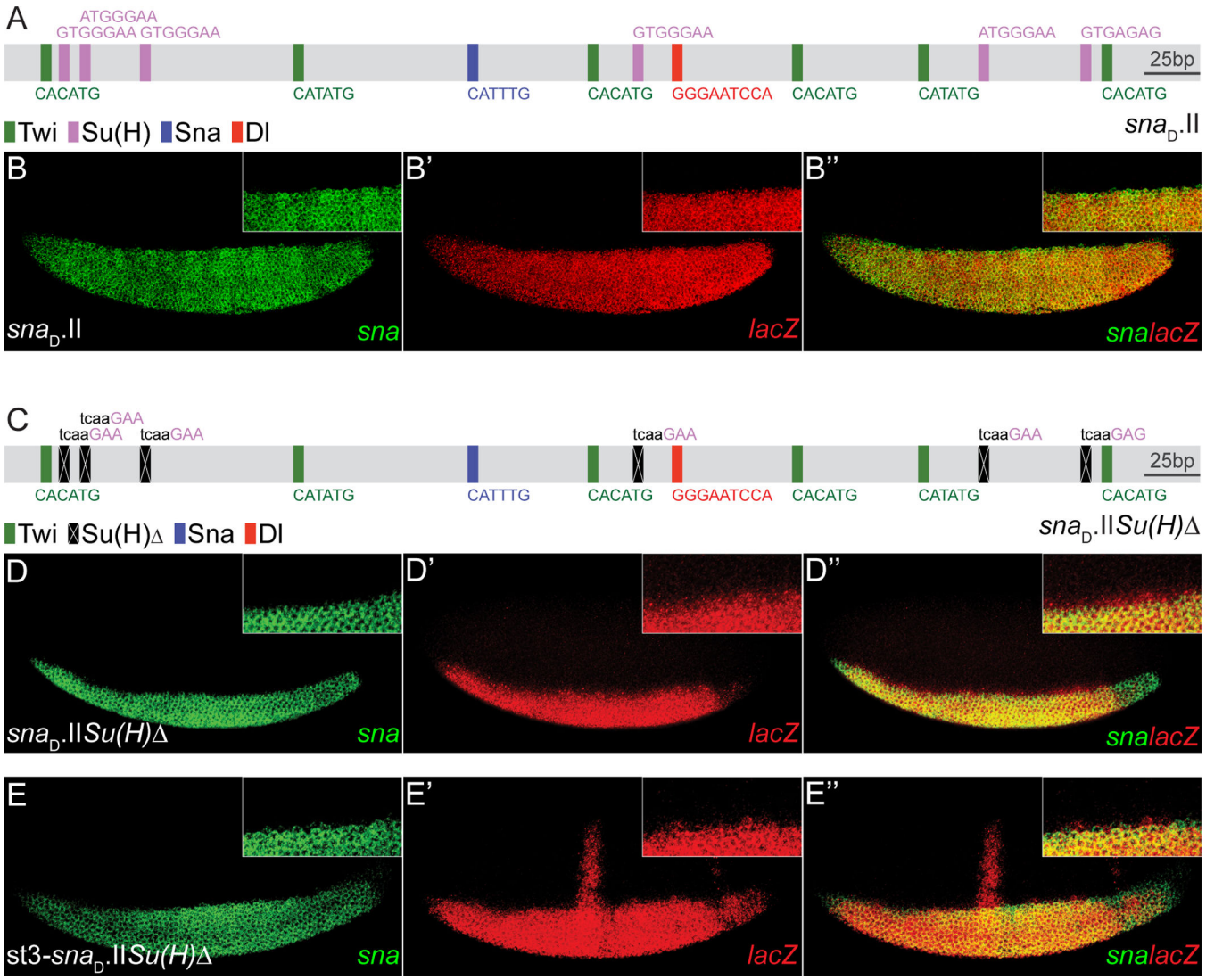

Figure 3. Su(H) binding sites support dorsal repression within a 567 bp minimal *sna* enhancer

(A,C) Schematics of an intact 567bp sna_D.II minimal enhancer (A; same as shown in Figure 2A except that location of Su(H) binding sites are added as magenta vertical boxes) or mutant version, sna_D.II*Su(H)*Δ, in which Su(H) binding sites are mutated (RTGRGAR>tcaaGAR). (B-B", D-D", E-E") Ventrolateral views of embryos processed by in situ hybridization using riboprobes to detect endogenous *sna* expression (green) and *lacZ* expression (red) supported by sna_D.II reporter construct (B,B'), sna_D.II *Su(H)*Δ reporter construct (D,D'), and chimeric st3-sna_D.II*Su(H)*Δ reporter construct (E,E'). Merged images showing overlap of endogenous *sna* and *lacZ* reporter expression domain (B'', D", E"). Insets are 2x magnifications of main embryo images showing relevant expression domains.

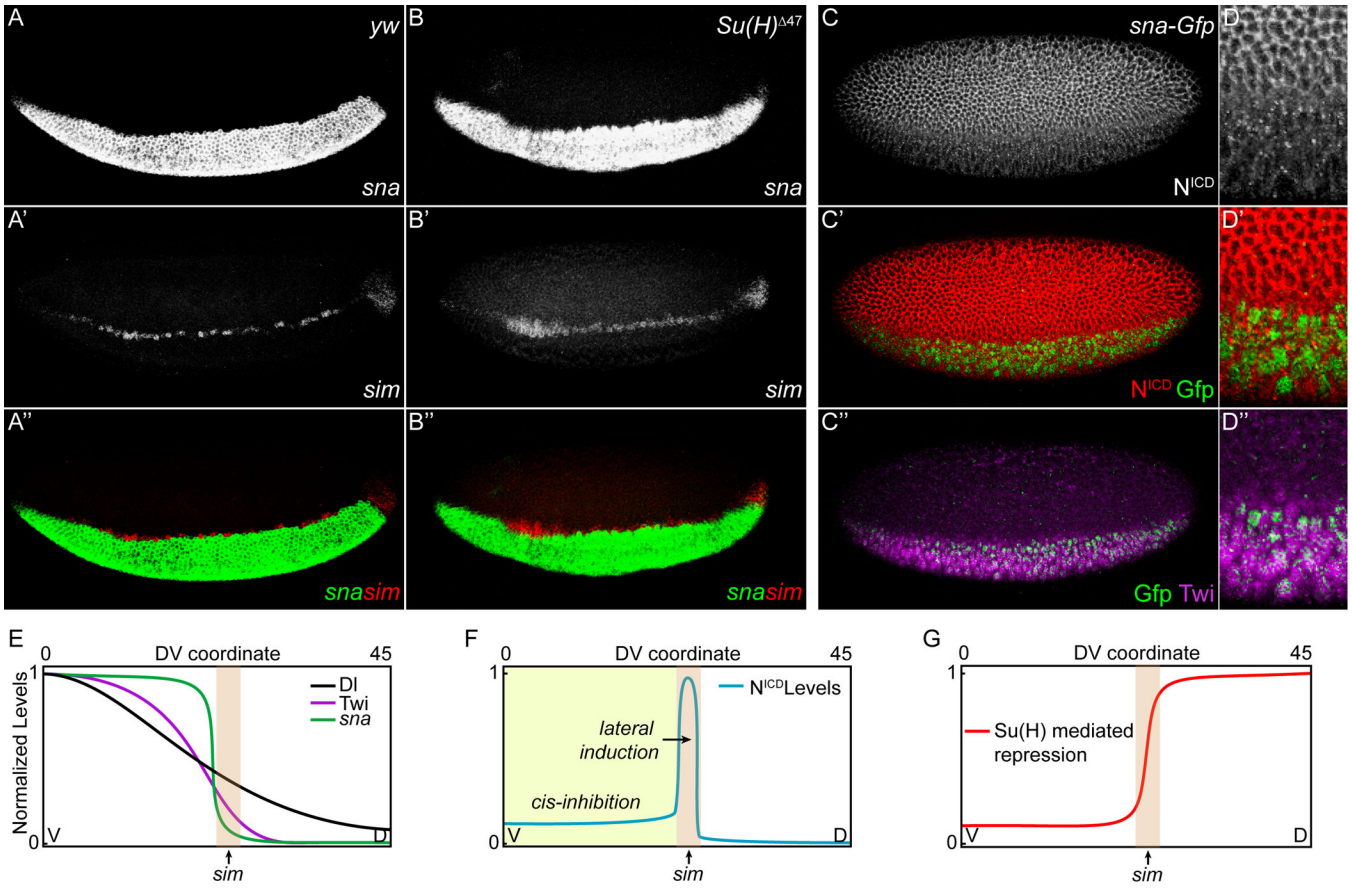

Figure 4. *Su(H)* mutants exhibit dorsal derepression of *sim* and *sna* genes

(A-A",B-B") Lateral view of a wildtype embryo (A-A") or a *Su(H)*$^{\Delta 47}$ mutant embryo (B-B") in which *sna* and *sim* transcripts were identified using respective riboprobes through multiplex in situ hybridization. (A,A') and (B'B') show individual gene expression patterns, whereas (A",B") show colocalization of *sna* (green) and *sim* (red).

(C-C") Colocalization of N^{ICD}, Gfp and Twi in a wildtype embryo expressing a *sna-Gfp* rescue construct (Dunipace et al., 2011), which allows localization of Sna-GFP protein using an anti-GFP antibody. Anti-N^{ICD} antibody was used to detect N^{ICD}, shown alone (C) or in combination with GFP (C': anti-N^{ICD} staining, red; anti-Gfp staining, green). Anti-Twi antibody was used to detect Twist expressing cells (C": anti-Twi, purple) relative to that of Snail (C": anti-GFP, green).

(D-D") 2x magnifications of similar domains from embryo staining shown in (C-C''). (E) A graphical representation of quantitative data for Dl, Twi and Sna nuclear gradients (Zinzen et al., 2006). Where *sim* expression domain is marked with a light brown box.

(F-G) Graphical models showing where our data supports an active Notch signaling domain (ventral regions; F) versus a Su(H) mediated repression domain (lateral and dorsal regions; G) using *sim* expression domain as a reference point for location along the DV axis of the *Drosophila* embryo.

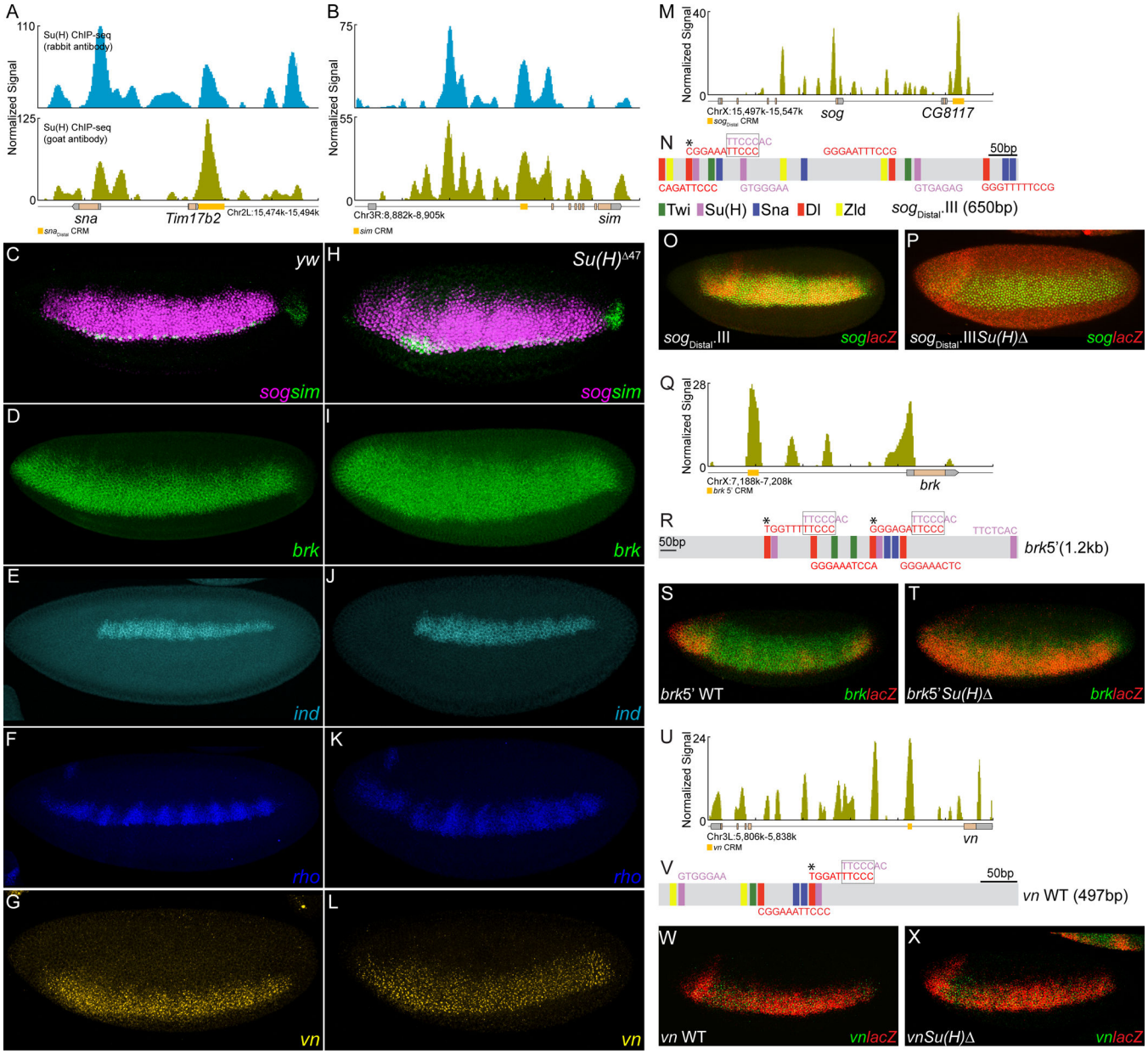

Figure 5. Mutant phenotypes and ChIP-seq analysis reveal a general DV patterning role for Su(H)

(A,B,M,Q,U) Su(H) ChIP-seq occupancy data in the vicinity of *sna* (A), *sim* (B), *sog* (M), *brk* (Q), and *vn* (U) gene loci. A graphical representation of each locus is shown with genomic coordinates at the bottom. Orange boxes highlight CRMs in which Su(H) binding sites were mutated in the current study or for the case of *sim*, Morel and Schweisguth, 2000. (C-L) Lateral views of widltype (C-G) or *Su(H)*$^{\Delta 47}$ mutant (H-L) embryos processed by fluorescent in situ hybridization using the following riboprobes: (C, H) *sog* (magenta) and *sim* (green); (D,I) *brk* (green); (E,J) *ind* (cyan); (F,K) *rho* (blue); and (G,L) *vn* (yellow). Images were pseudocolored in LSM software (Zeiss) for presentation.

(N,R,V) Schematics of three CRMs containing matches to the Su(H) binding site consensus: 650bp $sog_{D.}$III minimal enhancer (N, see also Figure S2J), 1.2 kb *brk*5' CRM (R), and 497bp *vn* CRM (V). "*" indicates a linked Dl-Su(H) binding site; the region of overlap is marked with a box around the sequence.

(O,P,S,T,W,X) Lateral views of embryos containing wildtype CRM *lacZ* reporter constructs (O,S,W) or versions containing mutations of Su(H) binding sites (P,T,X). Riboprobes were used to detect endogenous gene expression (green; *sog*, *brk*, or *vn*, as indicated) relative to that of *lacZ* expression (red) supported by the sog_{D}.III CRM (O,P), *brk5*' CRM (S,T), and *vn* CRM (W,X) wildtype versus mutant reporter constructs, respectively.

See also Figure S2.

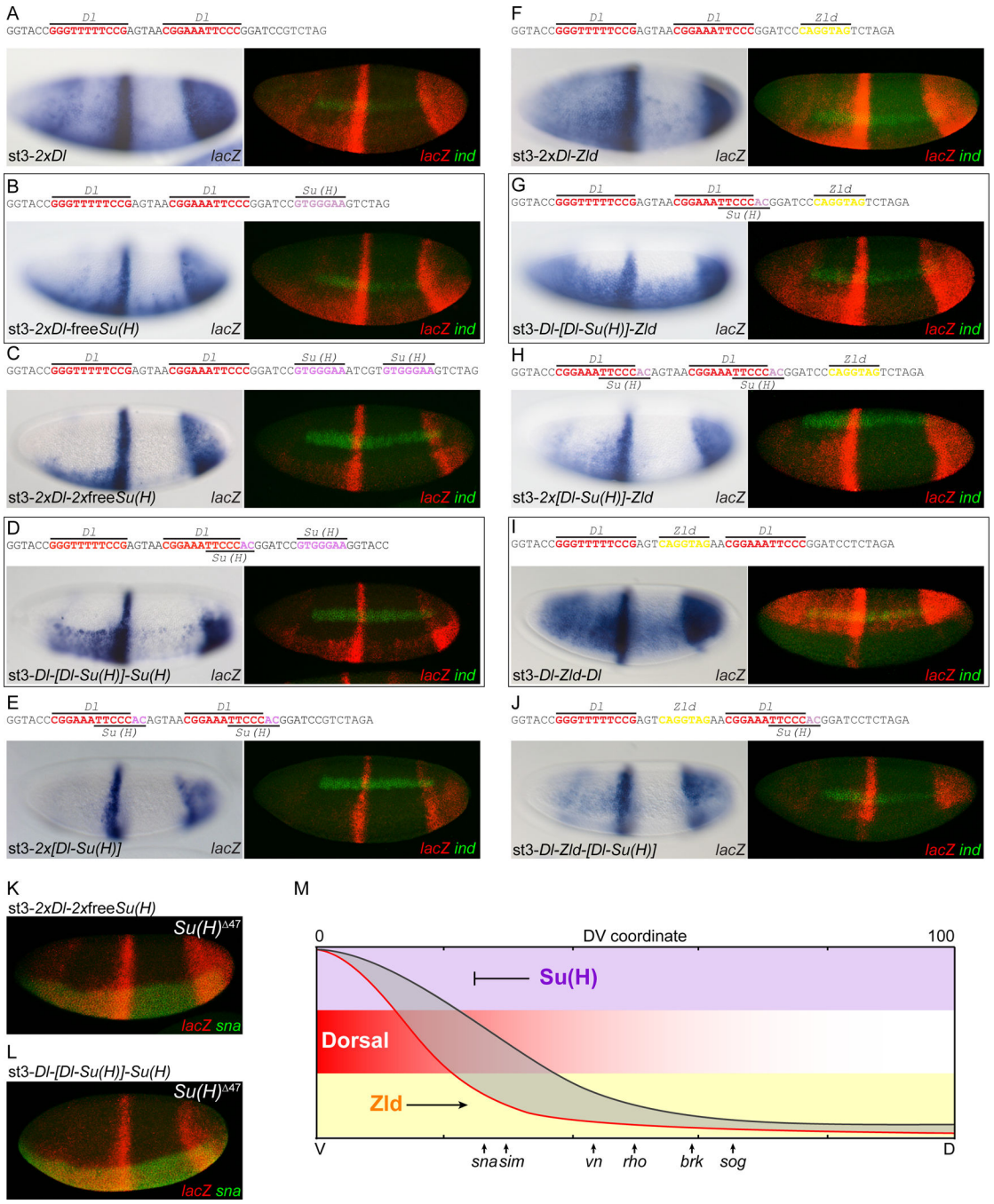

Figure 6. Synthetic reporter constructs recapitulate in vivo expression patterns of DV target genes

(A-J) Series of synthetic constructs containing different combinations of Dl, Su(H), and Zld binding sites. Sequence of each of the synthetic *lacZ* reporter constructs shown on top. On the bottom left are outputs supported by these reporter constructs assayed by in situ hybridization using a riboprobe to detect *lacZ* expression. On the right are ventrolateral views of embryos processed by multiplex in situ hybridization using riboprobes to detect both endogenous *ind* expression (green) and *lacZ* expression (red); embryos were processed equivalently and imaged under identical settings to allow direct comparisons of domains and

levels of expression. Embryos processed by multiplex in situ are also presented in Figures S3A–J; “rainbow palette” views are shown to provide information regarding levels of expression along the DV axis for the various constructs.

(K,L) Lateral views *Su(H)*$^{\Delta 47}$ mutant embryos expressing *2xDl-2xfreeSu(H)* (K) or *Dl-[Dl-Su(H)]-Su(H)* synthetic (L) processed by fluorescent in situ hybridization using riboprobes to *sna* (green) and *lacZ* (red).

(M) Su(H) mediated repression counterbalances activation through Dl and Zld. A graphical representation of quantitative data for Dl nuclear gradient (red line) (Reeves et al., 2012), with Zld and Su(H) ubiquitous expression domains represented by yellow and purple shading, respectively. Zld can extend the activation potential of the Dl gradient (black line), whereas Su(H) acts to inhibit it. Dorsal expression borders of *sna*, *sim*, *vn*, *rho*, *brk*, and *sog* are marked by arrows along the DV axis of the embryo (Reeves et al., 2012).

See also Figure S3.

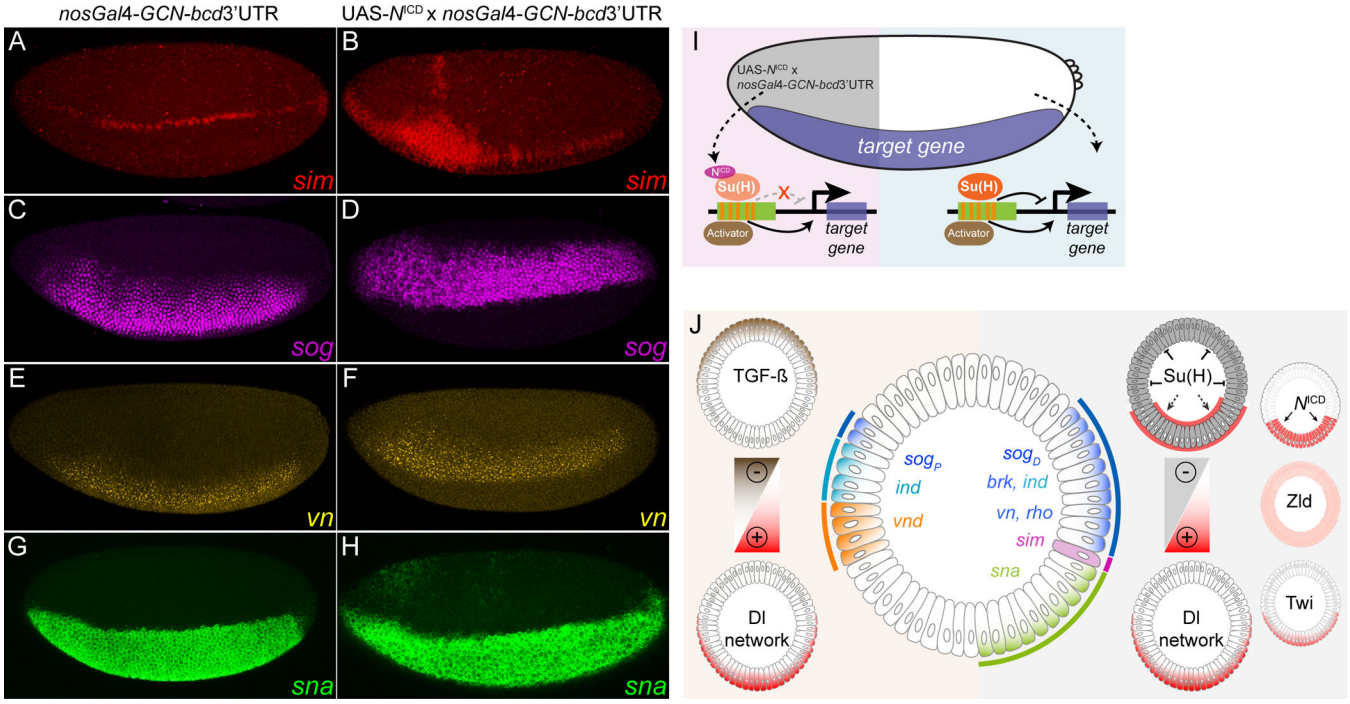

Figure 7. Ectopic expression of N^{ICD} results in expansion of the dorsal boundaries for many DV target genes

(A-H) Expression of genes *sim* (red; A,B), *sog* (magenta; C,D), *vn* (yellow; E,F), and *sna* (green; G,H) in control embryos, those containing only the *nosGal4-GCN-bcd3'*UTR Gal4 driver alone (A,C,E,G), or upon ectopic expression of the N^{ICD} domain at the anterior of the embryo (UAS-*N*^{ICD} x *nosGal4-GCN-bcd3'*UTR; B,D,F,H). Embryos were processed by in situ hybridization using riboprobes to detect endogenous expression of indicated genes.

(I) A graphical representation of the ectopic expression of N^{ICD} mediated by the *nosGal4 GCN bcd*3' UTR driver. N^{ICD} is ectopically expressed at the anterior half of the embryo (outlined as gray region in embryo drawing) and presumably acts as anti-repressor in this region.

(J) A graphical representation of how activation-repression balance may position expression boundaries along the entire DV axis. Embryo cross-sections depict domains of action for a number of activators (red) and repressors (brown/gray) acting to support genes expressed along the DV axis (e.g. sna: green, sim: purple, etc.). TGF-β signaling may act to counter-balance Dl network-mediated activation of select genes expressed in the presumptive neurogenic ectoderm such as *ind* and *vnd* (left side) (Crocker and Erives, 2013; Garcia and Stathopoulos, 2011); whereas, our data here is consistent with the view that Su(H) functions as a more general repressor acting in both ventrolateral and dorsal regions to set the dorsal borders for a number of genes expressed along the DV axis including *sna*, *sim*, *vn*, and *sog*.